ACS APPLIED MATERIALS & INTERFACES

Research Article

Cite This: ACS Appl. Mater. Interfaces 2018, 10, 3938−3947

www.acsami.org

Flexible and Hierarchically Structured Sulfur Composite Cathode Based on the Carbonized Textile for High-Performance Li−S Batteries

Peibo Gao,[†] Shixing Xu,[†] Zhangwei Chen,[‡] Xi Huang,[†] Zhihao Bao,*[,†] Changshi Lao,*[,‡] Guangming Wu,*[,†] and Yongfeng Mei[§]

[†]Shanghai Key Laboratory of Special Artificial Microstructure Materials and Technology, School of Physics Science and Engineering, Tongji University, Shanghai 200092, China

[‡]Additive Manufacturing Institute, College of Mechatronics and Control Engineering, Shenzhen University, Shenzhen 518060, China

[§]Department of Materials Science, Fudan University, Shanghai 200433, China

Supporting Information

ABSTRACT: Carbon hosts have been utilized to obtain composite cathodes with high sulfur loadings for Li−S batteries. However, the complicated synthesis process may hinder their practical applications. Their mechanical and electrochemical properties shall be further improved. Herein, a facile scalable dip-coating process is developed to synthesize a flexible composite cathode with a high sulfur loading. Via the process, a hybrid composed of carbon nanotubes, carbon black, sulfur, and titania nanoparticles is successfully conformally coated on the carbonized textile (c-textile). The formed flexible c-textile@S/TiO_2 cathodes with sulfur loadings of 1.5 and 3.0 mg cm^{-2} can deliver reversible discharge capacities of 860 and 659 mA h g^{-1} at 2 C, respectively. For the latter one, it can retain 94% of the initial capacity after 400 cycles with a high Coulombic efficiency (~96%). When its sulfur loading is further increased to 7.0 mg cm^{-2}, its areal capacity reaches 5.2 mA h cm^{-2}. Such excellent performance is ascribed to the synergy effect of the three-dimension conductive hierarchical pore structure and TiO_2 additive. They can physically and chemically entrap the soluble polysulfides in the composite cathode. The as-synthesized free-standing composite electrode is of low cost and a high areal capacity, making it suitable for flexible energy storage applications based on Li−S batteries.

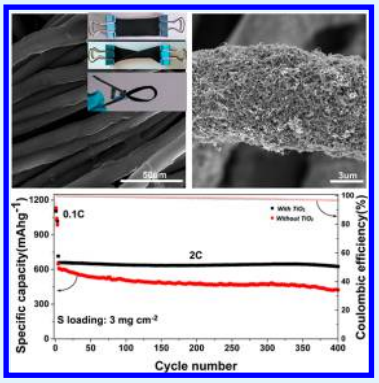

KEYWORDS: *carbonized textile, carbon nanotube, titania, dip coating, lithium−sulfur*

INTRODUCTION

Rechargeable batteries with high energy densities are very attractive for next-generation electric-energy storage systems and have great potentials in plug-in hybrids, portable electronic devices, and all-electric vehicles (EVs).[1] Among the existing devices, a lithium−sulfur (Li−S) battery has been considered one of the most promising candidates owing to its high theoretical energy density (2600 Wh kg^{-1}), low cost, and environmentally friendliness.[1−4] Despite these advantages, the Li−S battery is faced with several challenges. For example, the insulating nature of sulfur and reduction products (Li_2S_2 and Li_2S) reduces the utilization of the active materials.[5] The "shuttle effect" of the soluble polysulfides (PSs), the reaction intermediates (Li_2S_n, $4 \leq n \leq 8$), between the cathode and the anode can lead to the loss of active sulfur, rapid capacity decay, and low Coulombic efficiency.[6,7] Another failure mechanism is the large volumetric variation (~80%) of the sulfur electrode during the lithiation process, causing detachment of the active material from the conductive substrate/matrix.[8]

To address the aforementioned challenges, one effective strategy is to impregnate sulfur into the conductive hosts (porous carbon, graphene, conductive polymer, carbon fiber cloth, etc.).[9−12] Among them, the carbon nanotube (CNT) is one of the most promising candidates due to its high conductivity which can greatly improve the utilization and rate capability of sulfur cathodes.[13,14] Besides, pores inherent in CNTs or their self-assembled networks can provide reservoirs for the soluble intermediate PSs and accommodate the strain/stress due to the volume changes.[15−17] Additionally, CNTs have potential applications for the flexible electronic devices because of their outstanding mechanical properties.[18,19] Though the high sulfur loading could be achieved in CNT-based cathodes, their capacity retention and rate capability were not satisfying unless a high percentage (≥30 wt %) of CNTs was used.[20−24] Recently, there were breakthroughs on the high-loading sulfur cathodes by using thick carbon hosts with large and open pores.[8,25−27] For example, the sulfur/hollow carbon fiber foam electrode exhibited a high areal capacity of 12.0 mA h cm^{-2} with a sulfur loading of 16.5 mg cm^{-2}. The good performance was partially ascribed to the large pore volume in the foam. The volume could absorb a large amount of soluble PSs and electrolytes, which were essential for the long cycling

Received: October 24, 2017
Accepted: January 8, 2018
Published: January 8, 2018

DOI: 10.1021/acsami.7b16174
ACS Appl. Mater. Interfaces 2018, 10, 3938−3947

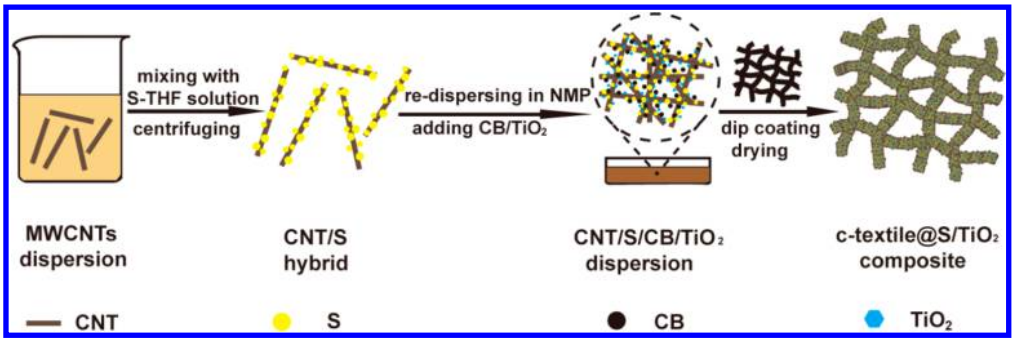

Figure 1. Schematic illustration of the structure and synthesis process of c-textile@S/TiO_2 composite.

stability of the high-loading sulfur cathode.[26] However, their thickness (~2 mm) might be detrimental to the initial packaging of Li−S batteries. Meanwhile, the flexibility and their energy density of the electrodes could be further improved. Additionally, most of the carbon hosts were nonpolar; therefore, they were ineffective to entrap the polar PSs. Recently, inspired by the concept of surface chemistry, many polar host materials (e.g., TiO_2, Co_3O_4, and metal−organic frameworks (MOFs))[28−31] were adopted to strengthen the affinity between PSs and the cathode composite, leading to improved electrochemical performance. Unfortunately, the conductivities of these materials were very low, which unavoidably compromised the rate capability. Overall, long-term (≥300 cycles) cyclability and high rate performance (≥2 C rate) were rarely demonstrated when the areal sulfur loading was higher than 3.0 mg cm^{-2}. Therefore, it is still a great challenge to improve the sulfur utilization and at the same time achieve satisfactory capacity for the high sulfur loading even at high current densities with good capacity retention. A feasible solution is to reduce the dimension of sulfur particles, enhance the uniform distribution of sulfur in the conductive carbon framework, and use polar metal oxides additive as PS immobilizer at the same time.[32]

Solution processing of CNTs was previously used to turn textile, paper, fabric, and sponge into conductive electrode materials for supercapacitors or current collectors.[33−35] However, to our knowledge, active materials together with carbon nanotubes have not been coated onto the textile materials to form the composite cathode for lithium ion batteries via the dip-coating process. Herein, we demonstrated a simple dip-coating and drying process to synthesize a flexible and robust three-dimensional (3D) composite cathode. It was composed of carbonized textile (c-textile), on which a carbon nanotube together with sulfur and titania nanoparticles was conformally coated. The formed c-textile@S/TiO_2 composite cathode could deliver a discharge capacity of 860 mA h g^{-1} at a current rate of 2 C, and a reversible specific capacity of 814 mA h g^{-1} was achieved at 4 C with sulfur loadings of 1.5 mg cm^{-2}. Remarkably, we further confirmed that the cathode retained superior cycling stability, corresponding to 94% capacity retention at 2 C after 400 cycles with sulfur loadings of 3.0 mg cm^{-2}. To our knowledge, such long-term cyclability at a high rate of 2 C was rarely reported when the areal sulfur loading was higher than 3.0 mg cm^{-2}. Additionally, the c-textile@S/TiO_2 composite cathode with 7.0 mg cm^{-2} sulfur loading delivered a high areal capacity of 5.2 mA h cm^{-2}, higher than the current commercial level (~3.0−4.0 mA h cm^{-2}). Such outstanding performance was ascribed to the hierarchical pore structure and conductive network of the composite sulfur cathode, together with chemical adsorption of TiO_2 on the soluble PSs.

EXPERIMENTAL SECTION

Synthesis of Carbonized Textile. The carbonization of bamboo textile was performed as previously reported.[36] Typically, a piece of commercially available bamboo textile was soaked in 50 mL of NaF solution and kept for 1 h. Then the textile was dried in an oven at 120 °C for 2 h. Finally, the NaF-treated bamboo textile was carbonized at 900 °C for 1 h in the tube furnace under an argon atmosphere. After being cooled to room temperature, the as-obtained carbonized textile was washed with distilled water several times and dried at 120 °C.

Synthesis of S/CNT Hybrid. Raw MWCNTs (30−50 nm, Chengdu, China) were dispersed into 1.0 wt % sodium dodecyl sulfate (SDS, AR) aqueous solution at a concentration of 1.0 mg/mL by combining vigorous stirring and sufficient ultrasonication to ensure a homogeneous CNT dispersion, while the sublimed sulfur (AR) was dissolved into tetrahydrofuran (THF) to get a precursor solution with a concentration of 0.30 M. The sulfur precursor solution was then added into CNT dispersion with vigorous stirring. The weight ratio of sulfur and MWCNTs was controlled as 90:5 in the mixture. CNT/S hybrid was separated and washed with distilled water three times by high-speed centrifugation. SDS was also removed in this washing process. Pure sulfur nanoparticles were prepared by the same method but without addition of MWCNTs.

Synthesis of c-textile@S and c-textitle@S/TiO_2 Cathodes. To synthesize c-textile@S, 190 mg (95 wt %) of CNT/S hybrid and 10 mg (5 wt %) of Super P were dispersed in 10 mL of NMP. Subsequently, c-textile was soaked into the dispersion and then taken out. After being dried at 60 °C overnight, c-textile@S composite was formed. The sulfur loading could be controlled by varying the times of soaking. The sulfur loading of the cathode could be calculated as follows

$$\text{sulfur loading} = (W_2 - W_1) \times 88\%$$

where W_1 and W_2 are the weights of c-textile before and after the dip-coating and drying process.

For preparation of c-textile@S/TiO_2 cathode, the percentages of raw materials were slightly adjusted as 92 wt % CNT/S, 5 wt % Super P carbon black, and 3 wt % TiO_2 (5−10 nm, Aladdin, Shanghai, China). The rest of the preparation procedures were the same. For comparison, 80 wt % of sulfur nanoparticles, 10 wt % of super P carbon black, and 10 wt % of PVDF binder were dispersed in NMP solution to form a slurry. The formed slurry was then spread onto a carbon-coated aluminum foil with the doctor-blading method, dried, and pressed to form the nano-S/CB/PVDF electrode with a sulfur loading of ~1.0 mg cm^{-2}.

Electrochemical Characterization. The electrodes were cut into round disks with a diameter of 12 mm with a corresponding area of 1.13 cm^2. The areal sulfur loading was in the range of 1.5−7.0 mg cm^{-2}, equivalent to a mass loading range of 1.7−7.9 mg. The electrodes, Li metal foil as anode, and Celgard 2400 membrane as separator were assembled into 2016-type coin cells inside an argon-filled glovebox. The used electrolyte was composed of 1 M

DOI: 10.1021/acsami.7b16174
ACS Appl. Mater. Interfaces 2018, 10, 3938−3947

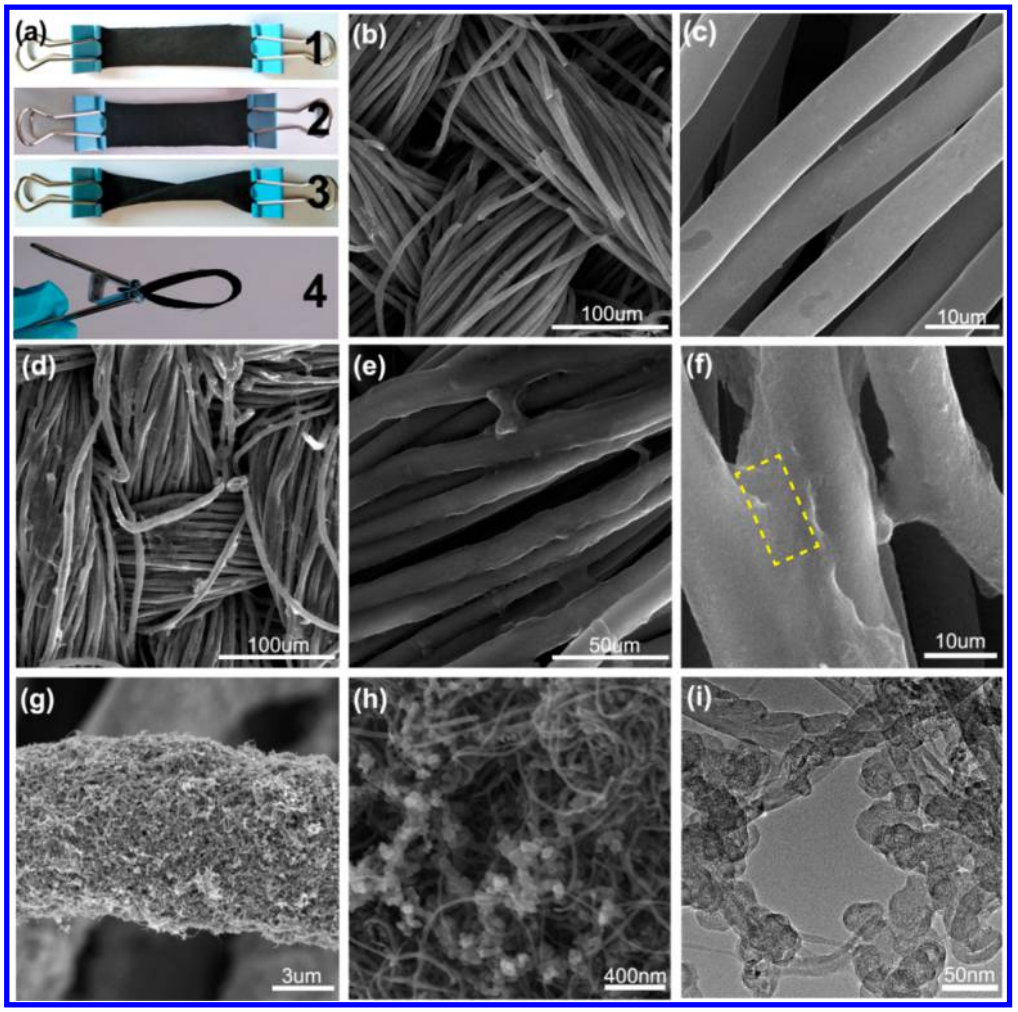

Figure 2. (a) Photographs of the obtained (1) c-textile and (2–4) c-textile@S/TiO_2 composite; (b, c) SEM images of the c-textile; (d–g) SEM images of the c-textile@S/TiO_2 composite with sulfur mass loading of 3.0 mg cm^{-2} (CNT bridging is marked in the yellow rectangle in f); (h and i) SEM and TEM images of the outside layer of a fiber in the composite, respectively.

bis(trifluoromethane) sulfonamide lithium salt (LiTFSI) with 1 wt % $LiNO_3$ dissolved in a mixture of 1,3-dioxolane (DOL) and dimethoxymethane (DME) (1:1 ratio, by volume). The amount of electrolyte in the coin cell with an areal sulfur loading of 1.5 mg cm^{-2} was 50 μL. When the areal sulfur loadings were increased to 3.0, 5.0, and 7.0 mg cm^{-2}, the corresponding amounts of electrolyte were 80, 130, and 160 μL, respectively. The galvanostatic discharge/charge measurements were conducted at a voltage range of 1.7–2.8 V using a Land battery test system (Land Electronic, Wuhan, China). The CV and EIS measurements were performed on an AutoLab 302N electrochemical workstation. The scan rate for CV measurements was set as 0.2 mV/s. The frequency range of EIS measurements was from 100 kHz to 0.01 Hz with an ac voltage amplitude of 5 mV.

Structure Characterization. A field-emission scanning electron microscope (FESEM, Philips XL30 FEG) and transmission electron microscope (TEM, JEOL JEM-2010) were used to characterize the morphologies and structures of the samples. Thermogravimetric analysis (TGA, Shimadzu DRG-60) was used to determine the content of each component in the hybrids. To measure the TiO_2 content in the CNT/S/CB/TiO_2 composite, TGA was performed in air flow, while the sulfur content in the CNT/S/CB composite was determined in N_2 flow.

RESULTS AND DISCUSSION

The synthesis process of the flexible composite cathode is illustrated in Figure 1. Sublimed sulfur was first dissolved into tetrahydrofuran to get a sulfur solution.[37] Meanwhile, mutiwalled CNTs (MWCNTs) with diameters of 30–50 nm were dispersed in the aqueous solution with sodium dodecyl sulfate (SDS) as a surfactant by ultrasonication.[34] Owing to the different solubility of sulfur in the solvents, sulfur particles precipitated from the solution and formed CNT/S mixture when the sulfur solution was added into CNT dispersion with continuous stirring.[18,38] The anchoring of sulfur particles on CNTs might be due to the hydrophobic nature of the two materials. CNT/S hybrid was then separated and dispersed in NMP solution with carbon black (CB) and titania to form the CNT/S/CB/TiO_2 hybrid dispersion for dip coating. Conductive c-textile as the host for dip coating was synthesized by heating the textile of bamboo textile at 900 °C for 1 h in argon. c-textile was then dipped in the CNT/S/CB/TiO_2 dispersion and dried to form the composite cathode (c-textile@S/TiO_2). The photographs of the obtained raw textile, c-textile, and c-textile@S/TiO_2 composite cathodes are shown in Figure S1a, S1b, and 2a, respectively. c-textile exhibited superior mechanical flexibility, allowing it to be bent, wrinkled, and kneaded (see Video S1 and Figure 2a). Scanning electron microscopy (SEM) images in Figure 2b and 2c showed the microstructure of c-textile. It remained the morphology of the textile, which was interwoven with bundles of the long fibers. The thickness of c-textile was estimated to be ~180 μm with an areal mass of 4.0–

DOI: 10.1021/acsami.7b16174
ACS Appl. Mater. Interfaces 2018, 10, 3938–3947

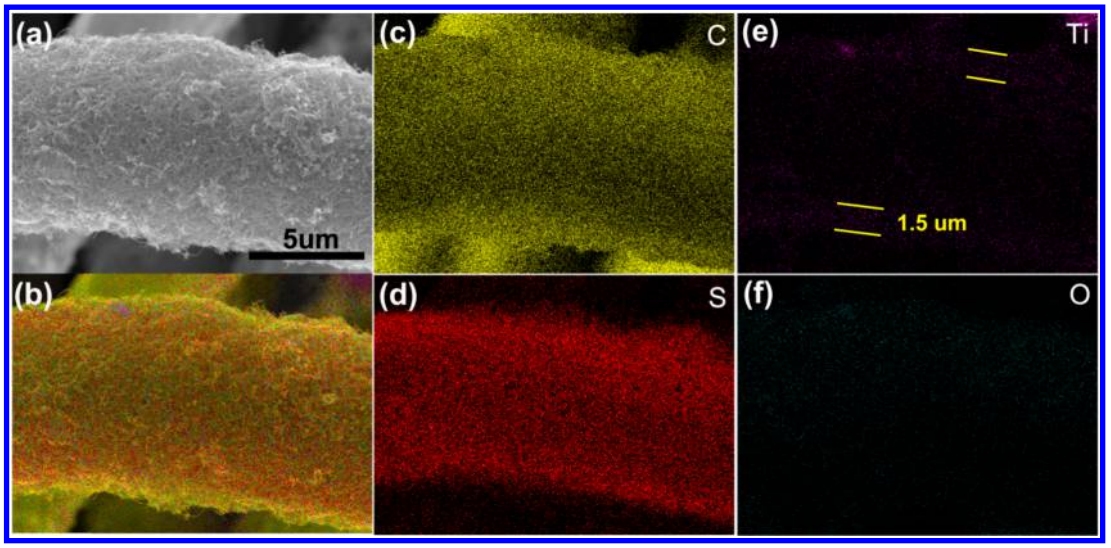

Figure 3. (a) SEM image of a fiber in the c-textile@S/TiO_2 composite cathode; (b) overlapped element mapping of the fiber and the corresponding element mapping images of (c) carbon, (d) sulfur, (e) titanium, and (f) oxygen.

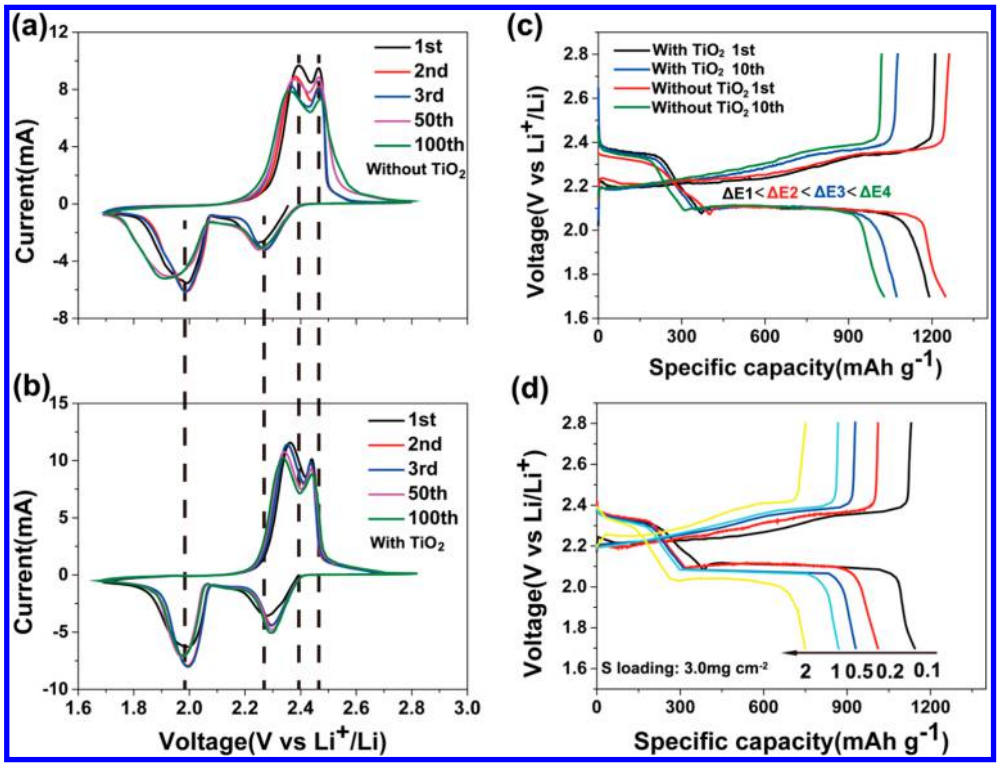

Figure 4. (a and b) CV profiles of the c-textile@S and c-textile@S/TiO_2 cathodes at the 1st, 2nd, 3rd, 50th, and 100th cycle, respectively; (c) galvanostatic discharge−charge profiles of the c-textile@S and c-textile@S/TiO_2 cathodes at 0.1 C; (d) galvanostatic discharge−charge profiles of the c-textile@S/TiO_2 cathode at the different current densities.

4.5 mg cm^{-2}. Its sheet resistance (R_s) was measured to be ∼1 Ω/sq. SEM images (Figure 2d−f) of the c-textile@S/TiO_2 composite cathode with sulfur mass loading of 3.0 mg cm^{-2} showed a similar morphology as that of c-textile. However, coarser morphology was observed in SEM and transmission electron microscopy (TEM) images (Figure 2g-2h) at higher magnifications. The outside layer of the fiber in the composite was of intertwined CNTs and sulfur nanoparticles with a size of 25−40 nm. The size was smaller than that of the sulfur nanoparticles from the solvent-exchange process without CNTs.[37] In the precipitation process, CNTs might provide the grafting sites and prevent the coalescence of sulfur nanoparticles.[39] It was surprising to find out that R_s only increased to ∼8 Ω/sq, considering the weight ratio of CNT:S was 5:90. The excellent electrical property of the composite was partially due to the CNT bridging between neighboring fibers, as shown in the yellow rectangular area in Figure 2f. The CNT/S/CB/TiO_2 hybrid was adhered tightly on c-textile. Only a very small fraction of CNTs was found to be peeled from the composite in the tape adhesion test (see Video S2). The excellent mechanical property of the composite cathode made it possible for roll-to-roll fabrication of the energy storage devices.

DOI: 10.1021/acsami.7b16174
ACS Appl. Mater. Interfaces 2018, 10, 3938−3947

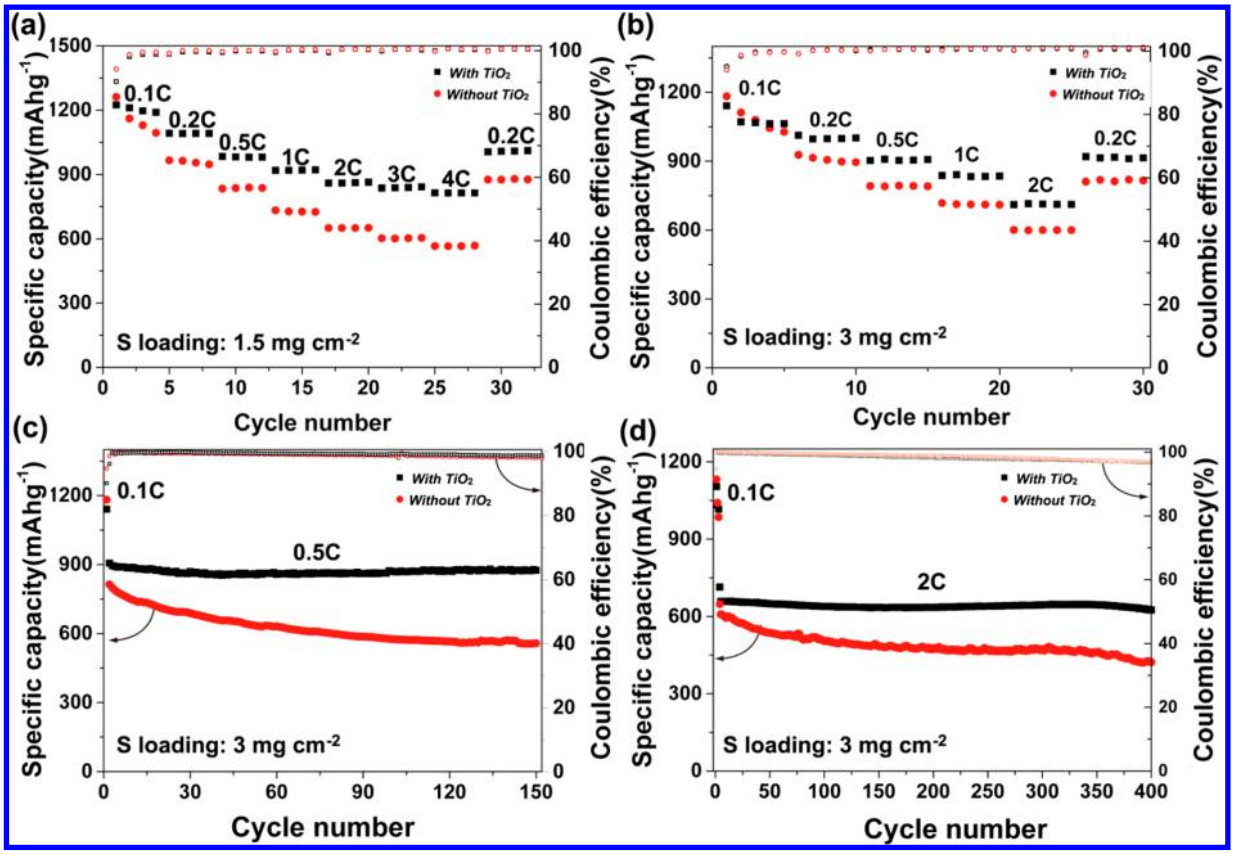

Figure 5. Rate performance of the c-textile@S/TiO_2 and c-textile@S cathodes with S loadings of (a) 1.5 and (b) 3.0 mg cm^{-2}; (c) cycling performance of these two cathodes with loading of 3.0 mg cm^{-2} at 0.5 C; (d) long cycling stability of these two cathodes with S loading of 3.0 mg cm^{-2} at 2 C.

Figure 2h shows that an open porous structure was formed in c-textile@S/TiO_2 composite, and no large sulfur agglomerates were found. TEM images (Figure 2i) of the outside layer of the fibers in the composite confirmed the good dispersion of sulfur nanoparticles, which were intimately anchored onto MWCNTs. The pores with a size of several tens to hundreds of nanometers among MWCNTs could be observed; however, no pore was measured in the fibers of textile, as indicated in its nitrogen absorption−desorption isotherms (Figure S2). The 3D macroporous structure inherited from the textile and the mesopores formed among CNTs composed the hierarchical pore structure in the composite. The structure was able to retain a large amount of the electrolyte and soluble PSs and facilitate the transport of lithium ions,[8,24,25,27,40] which was good for the high-power Li−S batteries. Recently, TiO_2 was found to be an efficient sulfur mediator, which could greatly enhance the electrochemical performance of sulfur cathode.[31,41−43]

In the current research, TiO_2 nanoparticles were also successfully incorporated in the intertwined MWCNTs by the dip-coating process, as confirmed by the element mapping images (Figure 3). The above result confirmed that the CNT/S/CB/TiO_2 hybrid was successfully conformally coated onto the long carbon fiber of c-textile. The self-assembly of conformal coating was due to the van der Waals force among the nanoparticles induced by evaporation of the solvent. From the Ti element image as shown in Figure 3e, the thickness of the conformal coating layer was roughly estimated to be ∼1.5 um. SEM analyses of the CNT/S/CB hybrids without (Figure S3a) and with TiO_2 (Figure S3c) additive revealed that introduction of tiania in the composite improved the distribution homogeneity of the sulfur nanoparticles. The sulfur contents in the hybrids were calculated to be 88% and 86% with thermogravimetric analyses (TGA; Figure S3b and S3d) of CNT/S/CB and CNT/S/CB/TiO_2 hybrids, respectively. The values were basically consistent with 90% and 87%, the determined sulfur percentages in the raw materials, respectively. Hence, the sulfur contents in the composite were calculated with the mass changes before and after the dipping and drying process together with the percentage of sulfur in the raw materials.

To evaluate the electrochemical performance of the composites, CR2016 coin cells with c-textile@S/TiO_2 and c-textile@S as cathodes were assembled and tested. Figure 4a shows the cyclic voltammetry (CV) profiles of the c-textile@S composites within a potential window of 1.7−2.8 V. Two well-defined reduction peaks in the cathodic scan were observed with a scan rate of 0.2 mV s^{-1}. The peak at ∼2.30 V corresponded to the conversion of element sulfur (S_8) to the high-order lithium polysulfide (e.g., Li_2S_x, $4 \le x \le 8$). The strong cathodic peak at ∼1.99 V suggested the further reduction of soluble polysulfides to solid-state Li_2S_2/Li_2S. In the subsequent anodic scan, two oxidation peaks existed distinctly at 2.39 and 2.46 V, suggesting the reversible conversion from Li_2S to PSs and from PSs to element S.[14,16,42,44] However, in the CV curves (Figure S4) of conventional S/CB/binder cathode, only one anodic current peak at 2.5 V could be detected during the initial three cycles. The appearance of a single peak was due to the increased electrode resistance and slower dynamics, which agreed with previous reports.[45−47] Large variation of the locations of the

DOI: 10.1021/acsami.7b16174
ACS Appl. Mater. Interfaces 2018, 10, 3938−3947

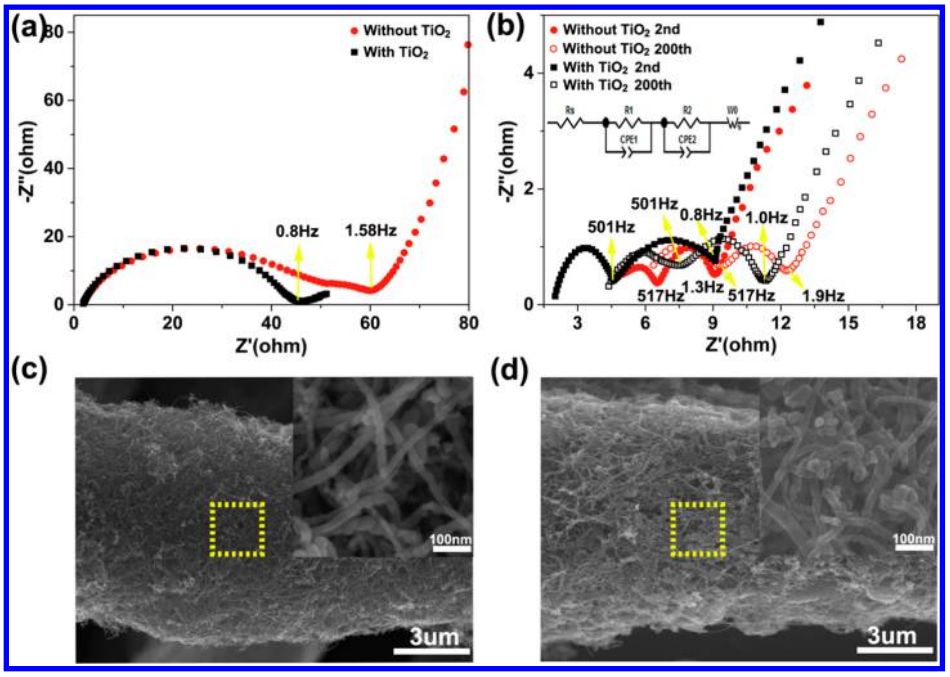

Figure 6. Electrochemical impedance spectra (a) before cycling, (b) after 2 and 200 cycles (inset was the fitted equivalent circuit.); SEM images of the c-textile@S/TiO_2 cathodes (c) before and (d) after 2 and 200 cycles, respectively (insets are magnified images of the rectangular areas).

anodic peaks for c-textile@S was observed in the subsequent cycles. This phenomenon was ascribed to the rearrangement of sulfur nanoparticles from their original positions to more energetically stable sites.[13,48−50] No significant changes appeared in the CV profile (Figure 4b) of the c-textile @S/TiO_2 cathode, implying TiO_2 facilitated the uniform distribution of active sulfur, as confirmed by Figure S3c. Moreover, compared with c-textile@S cathode, its cathodic peaks became stronger and exhibited a slight positive shift, whereas its anodic peaks gradually shifted to lower potentials, indicating a more facile redox activity.[49] The almost overlapped voltage profiles after 50 and 100 cycles for c-textile@S/TiO_2 cathode indicated that the addition of TiO_2 could enhance the stability of sulfur electrode. The anodic peak at 2.46 V related to the conversion from PS to element S became weaker (Figure 4b) because the electrostatic attraction existed between TiO_2 and PS and less PS was converted to sulfur.[42] It is consistent with its lower initial capacity shown in the initial galvanostatic discharge/charge curve (Figure 4c). The curves also indicated that the electrodes underwent a typical two-plateau behavior. The voltage hysteresis (ΔE) between the reduction and the oxidation plateau voltages for c-textile@S/TiO_2 cathode was smaller than with c-textile@S cathode, which indicated that the cell had a better reversibility and less polarization on c-textile@S/TiO_2 cathode.[51] Figure 4d shows the charge/discharge plots of c-textile@S/TiO_2 cycled at various current densities. Though the voltage hysteresis increased when current densities increased, its voltage hysteresis at each current density was smaller compared with that of the c-textile@S (Figure S5). The rate performance of the composite electrodes is shown in Figure 5a and 5b. The c-textile@S composite with a loading of 1.5 mg cm^{-2} delivered a high discharge capacity of 1262 mA h g^{-1} in the first cycle at 0.1 C, indicating easy electrochemical activation of sulfur owing to its nanosize and superior conductivity of the carbon network. Its capacity dramatically dropped in the following cycles. It was due to the loss of soluble PSs into the electrolyte because of the extremely high content (~88 wt %) of sulfur in the hybrid.[8,52−54] Contrary to c-textile@S, the composite with TiO_2 additive exhibited a slight capacity decay, even at 0.1 C, indicating that the TiO_2 effectively mitigated the dissolution of polysulfides into the organic electrolyte, which was further confirmed by the polysulfide affinity experiment. In the experiment, 5 mg of c-textile, CNT, and TiO_2 sample was added into three sealed glass vials containing lithium polysulfide (Li_2S_6, 0.1 M) in DOL/DME solvents (1:1 by volume, 5 mL). The blank PS solution was added in the vial with the same volume as a control. Also, two cells with c-textile@S and c-textile@S/TiO_2 composites as cathodes were cycled 5 times, and the composites were then taken out and immersed into 1,3-dioxolane (DOL) for 24 h in a glovebox. The images of the solutions with different samples are shown in Figure S6. The color of the solution with c-textile/S/TiO_2 was faint yellow and remained unchanged, similar to the solution containing TiO_2, while the color of the other solution was deeper. For c-textile@S and c-textile@S/TiO_2 composites with a sulfur loading of 1.5 mg cm^{-2}, the discharge capacities were 1161, 966, 834, 732, 650, 602, and 566 mA h g^{-1} and 1211, 1092, 984, 919, 860, 836, and 814 mA h g^{-1} at 0.1, 0.2, 0.5, 1, 2, 3, and 4 C, respectively, while for the two composites with a sulfur loading of 3.0 mg cm^{-2}, discharge capacities of 1111, 927, 791, 717, and 600 and 1071, 1012, 908, 841, and 710 mA h g^{-1} were obtained at 0.1, 0.2, 0.5, 1, and 2 C, respectively, as shown in Figure 5b. The rate capability of c-textile@S/TiO_2 was far better than c-textile@S. Such superior rate performance for the c-textile/S/TiO_2 cathode might benefit from the faster reaction kinetics and Li^+ transport in the hierarchical pore structure.[32] Moreover, for c-textile@S/TiO_2 with sulfur loadings of 1.5 and 3.0 mg cm^{-2}, reversible capacities of 1005 and 920 mA h g^{-1} were recovered when the specific current density was switched back to 0.2 C, indicating the high reversibility and stability of the composite electrode. The cycling stability of the composite electrode is shown in Figure 5c and 5d. With a sulfur loading of 3.0 mg cm^{-2}, c-textile@S/TiO_2 cathode delivered stable

DOI: 10.1021/acsami.7b16174
ACS Appl. Mater. Interfaces 2018, 10, 3938−3947

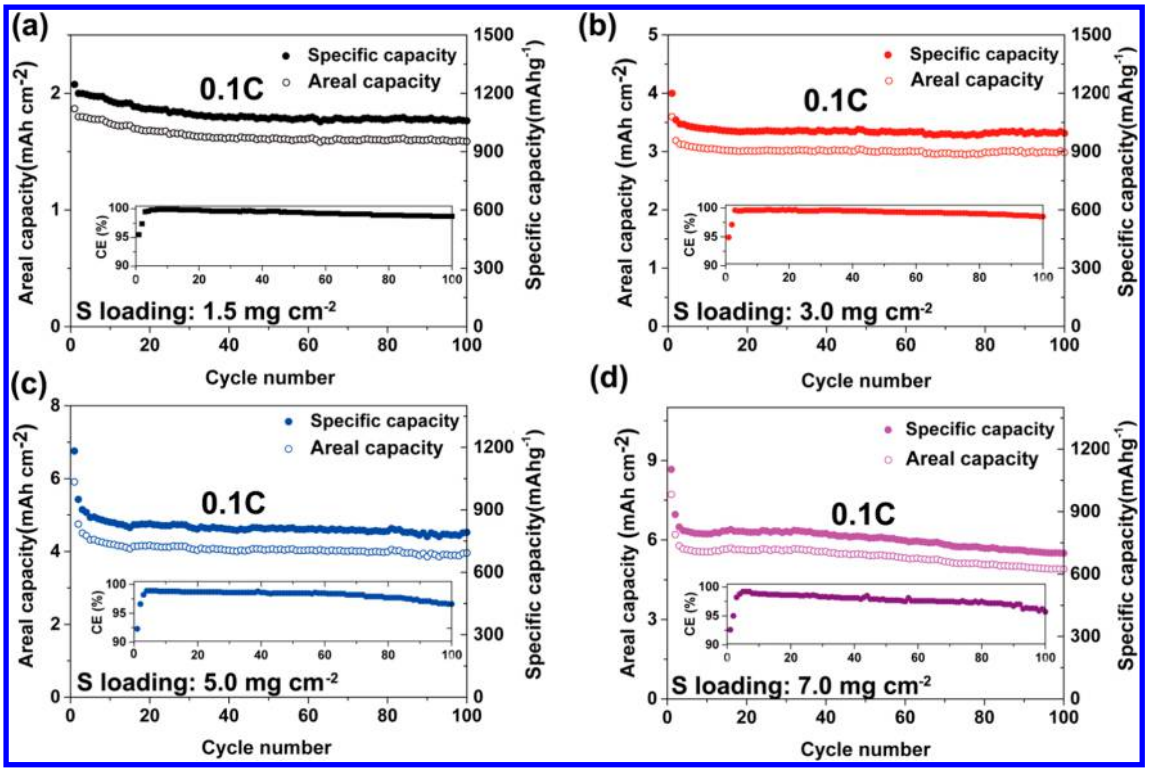

Figure 7. Cycling performance of the c-textile@S/TiO_2 cathode with sulfur areal loadings of (a) 1.5, (b) 3.0, (c) 5.0, and (d) 7.0 mg cm^{-2} (inset is the corresponding Coulombic efficiency).

capacities of 909 and 659 mA h g^{-1} at 0.5 and 2 C, respectively. After 150 and 400 cycles, 96% and 94% of the capacities were retained, corresponding to capacity decay rates of 0.026% and 0.013%, respectively. Moreover, the cathode exhibited high Coulombic efficiency (>96%), proving the good electrolyte absorbability of the hierarchical pore structure in the c-textile@S/TiO_2 and strong affinity between titania and PS. They could effectively suppress the shuttle effect and contribute to the cycling stability, which was confirmed by the polysulfide affinity study shown in Figure S6. For the composite electrodes without TiO_2, the capacity retentions were only 66% and 69% after 150 cycles at 0.5 C and 400 cycles at 2 C, corresponding to capacity decay rates of 0.205% and 0.076%, respectively. The performance of c-textile@S/TiO_2 was also superior to most of the sulfur cathodes based on thick carbon hosts as listed in Table S1. To better understand the mechanism for the improved electrochemical performance of c-textile@S/TiO_2 cathode, electrochemical impedance spectra analyses were conducted before and after cycling in the frequency from 0.01 to 100 kHz.

Nyquist plots (Figure 6a) of the c-textile@S/TiO_2 and c-textile@S electrodes before cycling displayed mainly a semicircle with a similar radius, which represented the charge transfer resistance (R_{ct}) at the high−medium-frequency region.[26,55,56] After the initial activation process for both electrodes, an additional semicircle appeared in the medium-frequency region. It was related with the formation of the passivation films on the electrode.[57−60] The equivalent circuit shown as the inset in Figure 6b was used to fit the Nyquist plots, and the fitting parameters are summarized in Table S2. Before the cycling, R_{ct} were 41.02 and 44.09 Ω for c-textile@S/TiO_2 and c-textile@S electrodes, respectively. However, after 2 cycles, the values dramatically decreased to 2.48 and 2.80 Ω. It was ascribed to the appearance of the soluble PSs, which was already confirmed by the color of the solution shown in Figure S6. The electrolyte resistances (R_s) for c-textile@S/TiO_2 were smaller than that for c-textile@S because there was less PS in the cells with the former one as the cathode. The appearance of PS could increase the viscosity of the electrolyte. Much smaller variation in the fitting parameters of R_1 and R_2 for Nyquist plots of c-textile@S/TiO_2 after 2 cycles and 200 cycles indicated more stable charge transfer and interface in the composite compared with c-textile@S. It was responsible for the highly stable performance of the composite.[57,61] EIS measurements were also carried out at different discharge and charge states during the second cycle at 0.1 C after the initial activation (Figure S7). Among all states, R_{ct} reached the maximum at the end of discharge, indicating that a considerable amount of soluble species had transferred to Li_2S/Li_2S_2 at the cutoff voltage of 1.7 V. It was also worth noting that the R_{ct} value decreased first and then increased during the charge process, indicating that most of the insoluble Li_2S/Li_2S_2 could be transferred to soluble polysulfides since polysulfides facilitated the charge thansfer.[30] After furthur charging, partial polysulfides were converted to insulating sulfur, consistent with analyses of CV plots. Figure 6c and 6d shows the morphologies of the c-textile@S/TiO_2 electrode before and after 200 cycles, respectively. The 3D porous network was retained well, and the blockage of the pore was not severe. SEM images (Figure S8a and S8b) of cross sections of the electrodes showed that their thickness almost did not change. It indicated that the carbon host reported here was stable. As shown in Figure 7a and 7b, although the capacities of c-textile@S/TiO_2 could reach 1058 and 1003 mA h g^{-1} for the cathodes with sulfur loadings of 1.5 and 3.0 mg cm^{-2}, respectively, their corresponding areal capacities were 1.6 and 3.0 mA h cm^{-2}, lower than the current commercial level (~3.0−4.0 mA h cm^{-2}).[40,62] To reach the level, electrodes with sulfur loading of 5.0 and 7.0 mg cm^{-2}

DOI: 10.1021/acsami.7b16174
ACS Appl. Mater. Interfaces 2018, 10, 3938−3947

were fabricated and tested. The sulfur loading, electrode thickness, and areal density were measured and are summarized in Figure S9. The results showed that the thickness of the cathode had a negligible increase. They exhibited initial specific capacities of 1185 and 1065 mA h g^{-1} at 0.05 C and retained capacities of 802 and 731 mA h g^{-1} after 100 cycles at 0.1 C, respectively. They corresponded to areal capacities of 4.0 and 5.2 mA h cm^{-2}, respectively. The electrolyte/sulfur (E/S) in this work was in the range of 20−29 ul/mg. The high E/S ratios also were used in the other porous structured cathodes.[25,63] It was believed that every space among fibers and CNTs should be partially filled with the electrolyte to guarantee good electrochemical performance. Moreover, for the electrodes with a sulfur loading of 5 and 7 mg cm^{-2}, their structures became compact, as confirmed by Figure S9. The compact structure not only lowered the amount of electrolyte but also contributed to the high volumetric capacity.[64] Although the E/S ratio decreased from 29 to 20 μL/mg as sulfur loading increased, the electrochemical performance was not affected by the ratio change, as confirmed by the negligible change of the initial capacity in Figure S10. Additionally, the determined sulfur and TiO_2 contents in the cathode are summarized in Table S3. The values fitted well with TGA analysis (Figure S11). The sulfur content in the cathode greatly increased with increasing sulfur loading, which could somehow increase the high energy density of Li−S batteries.

The above superior electrochemical performance of composite electrodes could be attributed to their hierachical structures formed in the dip-coating and drying process. The microscale fibers in c-textile built a 3D interconnected conductive network as the main channels for the transport of electrons, while nanoscale CNTs could intimately contact with sulfur nanoparticles, facilitating the transfer of electrons. Such hierarchical conductive network made the high rate capability and high utilization of active materials possible. Meanwhile, the macropores among fibers of c-textile could absorb large amounts of electrolytes, while the mesopores among CNT could accommodate the volume expansion and keep the soluble sulfide well localized. The hierarchical pore structure could enhance the transport of the lithium ions and further improve the Columbic efficiency, rate capability, and long-term cycling performance. In addition to the physical entrapment of soluble PS with pores, a small fraction (<5 wt %) of titania additive could chemically adsorb PS and enhanced the uniformity of sulfur nanoparticles in the conductive matrix. Although such synergy effect promoted the stable redox activity and greatly improved the electrochemical properties during the discharge/charge process of the composite electrode, some crucial issues remain to be resolved. The insulator nature and strong affinity of TiO_2 reduced the initial capacity, as confirmed by Figure 4c. Hence, the oxide type and percentage can be adjusted to reduce shuttle effect for better chemical entrapment of soluble polysulfide species and improve the initial capacity and Coulombic efficiency simultaneously. For example, VO_x is found to be an excellent sulfur immobilizer,[28] which can be tried in future work. Moreover, the textile can be directly conformally coated with CNT via dip coating in CNT dispersion and become the conductive matrix.[33] The conductive textile will be then turned into cathode materials with sulfur as active material via the process reported in this paper.

CONCLUSIONS

In summary, we designed and synthesized flexible sulfur composite cathode, c-texitle@S/TiO_2, with a hierarchical structure via a simple dip-coating process. In the process, carbon nanotube, carbon black, sulfur, and titania nanoparticle were successfully conformally coated on carbonized textile. The formed c-textile@S/TiO_2 cathode with a sulfur areal loading of 1.5 mg cm^{-2} delivered specific capacities of ∼860, 836, and 814 mA h g^{-1} at 2, 3, and 4 C, respectively. Impressively, the electrode with a loading of 3.0 mg cm^{-2} displayed a reversible capacity of 659 mA h g^{-1} at 2 C with a high capacity retention of 94% after 400 cycles. Its areal capacity reached 5.2 mA h cm^{-2} when its sulfur loading was further increased to 7.0 mg cm^{-2}. Such excellent performance was ascribed to hierarchical pore structure and conductive networks and TiO_2 in composite cathode. The as-synthesized free-standing composite electrodes are of low cost and have high areal capacities, making them suitable for flexible energy storage applications based on Li−S batteries.

ASSOCIATED CONTENT

Supporting Information

The Supporting Information is available free of charge on the ACS Publications website at DOI: 10.1021/acsami.7b16174.

Photographs of the raw textile and carbonized textile, SEM and TGA analysis of the CNT/S/CB hybrid and CNT/S/CB/TiO_2 hybrid, CV profiles of the S/CB/binder, galvanostatic discharge−charge profile of c-textile@S cathode, images of the solution with the electrodes, gavanostatic profiles, and Nyquist plots at different discharge/charge states of the c-textile@S/TiO_2, SEM images of the cross-section of the electrode, compassion of various flexible Li−S systems, list of fitting parameters of the equivalent circuit (PDF)

Video showing the superior mechanical flexibility test of the c-textile@S/TiO_2 electrode (AVI)

Video showing the tape adhesion test of the c-textile@S/TiO_2 electrode (AVI)

AUTHOR INFORMATION

Corresponding Authors

*E-mail: zbao@tongji.edu.cn.
*E-mail: cslao@szu.edu.cn.
*E-mail: wugm@tongji.edu.cn.

ORCID

Zhihao Bao: 0000-0002-8708-7510
Yongfeng Mei: 0000-0002-3314-6108

Author Contributions

The manuscript was written through contributions of all authors. All authors have given approval to the final version of the manuscript.

Notes

The authors declare no competing financial interest.

ACKNOWLEDGMENTS

This work was supported by the National Natural Science Foundation of China-Xinjiang Joint Fund (U1503292) and the National Natural Science Foundation of China (21271140).

DOI: 10.1021/acsami.7b16174
ACS Appl. Mater. Interfaces 2018, 10, 3938−3947

REFERENCES

(1) Bruce, P.; Freunberger, S.; Hardwick, L.; Tarascon, J. Li-O_2 and Li-S Batteries with High Energy Storage. *Nat. Mater.* **2011**, *11*, 19−29.
(2) Yamin, H.; Peled, E. Electrochemistry of a Nonaqueous Lithium/sulfur Cell. *J. Power Sources* **1983**, *9*, 281−287.
(3) Wang, D.; Zeng, Q.; Zhou, G.; Yin, L.; Li, F.; Cheng, H.; Gentle, I.; Lu, G. Carbon−sulfur Composites for Li−S Batteries: Status and Prospects. *J. Mater. Chem. A* **2013**, *1*, 9382−9394.
(4) Liang, J.; Sun, Z.; Li, F.; Cheng, H. Carbon Materials for Li−S Batteries: Functional Evolution and Performance Improvement. *Energy Storage Materials* **2016**, *2*, 76−106.
(5) Ji, X.; Nazar, L. Advances in Li−S Batteries. *J. Mater. Chem.* **2010**, *20*, 9821−9826.
(6) Rauh, R.; Shuker, F.; Marston, J.; Brummer, S. Formation of Lithium Polysulfides in Aprotic Media. *J. Inorg. Nucl. Chem.* **1977**, *39*, 1761−1766.
(7) Mikhaylik, Y.; Akridge, J. Polysulfide Shuttle Study in the Li/S Battery System. *J. Electrochem. Soc.* **2004**, *151*, A1969−A1976.
(8) Elazari, R.; Salitra, G.; Garsuch, A.; Panchenko, A.; Aurbach, D. Sulfur-impregnated Activated Carbon Fiber Cloth as a Binder-free Cathode for Rechargeable Li-S Batteries. *Adv. Mater.* **2011**, *23*, 5641−5644.
(9) Li, Z.; Jiang, Y.; Yuan, L.; Yi, Z.; Wu, C.; Liu, Y.; Strasser, P.; Huang, Y. A Highly Ordered Meso@Microporous Carbon-Supported Sulfur@Smaller Sulfur Core-Shell Structured Cathode for Li-S Batteries. *ACS Nano* **2014**, *8*, 9295−9303.
(10) Fang, R.; Zhao, S.; Pei, S.; Qian, X.; Hou, P.; Cheng, H.; Liu, C.; Li, F. Toward More Reliable Lithium-Sulfur Batteries: An All-Graphene Cathode Structure. *ACS Nano* **2016**, *10*, 8676−8682.
(11) Ji, X.; Lee, K.; Nazar, L. A Highly Ordered Nanostructured Carbon-sulphur Cathode for Lithium-sulphur Batteries. *Nat. Mater.* **2009**, *8*, 500−506.
(12) Li, W.; Zhang, Q.; Zheng, G.; Seh, Z.; Yao, H.; Cui, Y. Understanding the Role of Different Conductive Polymers in Improving the Nanostructured Sulfur Cathode Performance. *Nano Lett.* **2013**, *13*, 5534−5540.
(13) Xiao, Z.; Yang, Z.; Nie, H.; Lu, Y.; Yang, K.; Huang, S. Porous Carbon Nanotubes Etched by Water Steam for High-rate Large-capacity Lithium−sulfur Batteries. *J. Mater. Chem. A* **2014**, *2*, 8683−8689.
(14) Peng, H.; Huang, J.; Zhao, M.; Zhang, Q.; Cheng, X.; Liu, X.; Qian, W.; Wei, F. Nanoarchitectured Graphene/CNT@Porous Carbon with Extraordinary Electrical Conductivity and Interconnected Micro/Mesopores for Lithium-Sulfur Batteries. *Adv. Funct. Mater.* **2014**, *24*, 2772−2781.
(15) Chen, J.; Zhang, Q.; Shi, Y.; Qin, L.; Cao, Y.; Zheng, M.; Dong, Q. A Hierarchical Architecture S/MWCNT Nanomicrosphere with Large Pores for Lithium Sulfur Batteries. *Phys. Chem. Chem. Phys.* **2012**, *14*, 5376−5382.
(16) Sun, L.; Li, M.; Jiang, Y.; Kong, W.; Jiang, K.; Wang, J.; Fan, S. Sulfur Nanocrystals Confined in Carbon Nanotube Network as a Binder-free Electrode for High-performance Lithium Sulfur Batteries. *Nano Lett.* **2014**, *14*, 4044−4049.
(17) Zu, C.; Fu, Y.; Manthiram, A. Highly Reversible Li/dissolved Polysulfide Batteries with Binder-free Carbon Nanofiber Electrodes. *J. Mater. Chem. A* **2013**, *1*, 10362−10367.
(18) Jin, K.; Zhou, X.; Zhang, L.; Xin, X.; Wang, G.; Liu, Z. Sulfur/Carbon Nanotube Composite Film as a Flexible Cathode for Lithium−Sulfur Batteries. *J. Phys. Chem. C* **2013**, *117*, 21112−21119.
(19) Kang, H.; Sun, Y. Freestanding Bilayer Carbon-Sulfur Cathode with Function of Entrapping Polysulfide for High Performance Li-S Batteries. *Adv. Funct. Mater.* **2016**, *26*, 1225−1232.
(20) Yuan, Z.; Peng, H.; Huang, J.; Liu, X.; Wang, D.; Cheng, X.; Zhang, Q. Hierarchical Free-Standing Carbon-Nanotube Paper Electrodes with Ultrahigh Sulfur-Loading for Lithium-Sulfur Batteries. *Adv. Funct. Mater.* **2014**, *24*, 6105−6112.
(21) Zhou, G.; Wang, D.; Li, F.; Hou, P.; Yin, L.; Liu, C.; Lu, G.; Gentle, I.; Cheng, H. A Flexible Nanostructured Sulphur−carbon Nanotube Cathode with High Rate Performance for Li-S Batteries. *Energy Environ. Sci.* **2012**, *5*, 8901−8906.
(22) Huang, J.; Peng, H.; Liu, X.; Nie, J.; Cheng, X.; Zhang, Q.; Wei, F. Flexible All-carbon Interlinked Nanoarchitectures as Cathode Scaffolds for High-rate Lithium−Sulfur Batteries. *J. Mater. Chem. A* **2014**, *2*, 10869−10875.
(23) Song, J.; Gordin, M.; Xu, T.; Chen, S.; Yu, Z.; Sohn, H.; Lu, J.; Ren, Y.; Duan, Y.; Wang, D. Strong Lithium Polysulfide Chemisorption on Electroactive Sites of Nitrogen-Doped Carbon Composites For High-Performance Lithium−Sulfur Battery Cathodes. *Angew. Chem., Int. Ed.* **2015**, *54*, 4325−4329.
(24) Peng, H.; Xu, W.; Zhu, L.; Wang, D.; Huang, J.; Cheng, X.; Yuan, Z.; Wei, F.; Zhang, Q. 3D Carbonaceous Current Collectors: The Origin of Enhanced Cycling Stability for High-Sulfur-Loading Lithium-Sulfur Batteries. *Adv. Funct. Mater.* **2016**, *26*, 6351−6358.
(25) Miao, L.; Wang, W.; Yuan, K.; Yang, Y.; Wang, A. A Lithium-sulfur Cathode with High Sulfur Loading and High Capacity Per Area: a Binder-free Carbon Fiber Cloth-sulfur Material. *Chem. Commun. (Cambridge, U. K.)* **2014**, *50*, 13231−13234.
(26) Fang, R.; Zhao, S.; Hou, P.; Cheng, M.; Wang, S.; Cheng, H.; Liu, C.; Li, F. 3D Interconnected Electrode Materials with Ultrahigh Areal Sulfur Loading for Li-S Batteries. *Adv. Mater.* **2016**, *28*, 3374−3382.
(27) Chung, S.; Chang, C.; Manthiram, A. A Carbon-Cotton Cathode with Ultrahigh-Loading Capability for Statically and Dynamically Stable Lithium-Sulfur Batteries. *ACS Nano* **2016**, *10*, 10462−10470.
(28) Liang, X.; Kwok, C.; Lodi-Marzano, F.; Pang, Q.; Cuisinier, M.; Huang, H.; Hart, C.; Houtarde, D.; Kaup, K.; Sommer, H.; Brezesinski, T.; Janek, J.; Nazar, L. Tuning Transition Metal Oxide-Sulfur Interactions for Long Life Lithium Sulfur Batteries: The "Goldilocks" Principle. *Adv. Energy Mater.* **2016**, *6*, 1501636.
(29) Liang, Z.; Zheng, G.; Li, W.; Seh, Z.; Yao, H.; Yan, K.; Kong, D.; Cui, Y. Sulfur Cathodes with Hydrogen Reduced Titanium Dioxide Inverse Opal Structure. *ACS Nano* **2014**, *8*, 5249−5256.
(30) Zhou, J.; Li, R.; Fan, X.; Chen, Y.; Han, R.; Li, W.; Zheng, J.; Wang, B.; Li, X. Rational Design of a Metal−organic Framework Host for Sulfur Storage in Fast, Long-cycle Li−S Batteries. *Energy Environ. Sci.* **2014**, *7*, 2715−2724.
(31) Evers, S.; Yim, T.; Nazar, L. Understanding the Nature of Absorption/Adsorption in Nanoporous Polysulfide Sorbents for the Li−S Battery. *J. Phys. Chem. C* **2012**, *116*, 19653−19658.
(32) Li, Z.; Zhang, J.; Lou, X. Hollow Carbon Nanofibers Filled with MnO_2 Nanosheets as Efficient Sulfur Hosts for Lithium-Sulfur Batteries. *Angew. Chem., Int. Ed.* **2015**, *54*, 12886−12890.
(33) Hu, L.; Pasta, M.; La Mantia, F.; Cui, L.; Jeong, S.; Deshazer, H.; Choi, J.; Han, S.; Cui, Y. Stretchable, Porous, and Conductive Energy Textiles. *Nano Lett.* **2010**, *10*, 708−714.
(34) Hu, L.; Choi, J.; Yang, Y.; Jeong, S.; La Mantia, F.; Cui, L.; Cui, Y. Highly Conductive Paper for Energy-storage Devices. *Proc. Natl. Acad. Sci. U. S. A.* **2009**, *106*, 21490−21494.
(35) Chen, W.; Rakhi, R.; Hu, L.; Xie, X.; Cui, Y.; Alshareef, H. High-performance Nanostructured Supercapacitors on a Sponge. *Nano Lett.* **2011**, *11*, 5165−5172.
(36) Bao, L.; Li, X. Towards Textile Energy Storage from Cotton T-Shirts. *Adv. Mater.* **2012**, *24*, 3246−3252.
(37) Jia-jia, C.; Xin, J.; Qiu-jie, S.; Chong, W.; Qian, Z.; Ming-sen, Z.; Quan-feng, D. The Preparation of Nano-sulfur/MWCNTs and Its Electrochemical Performance. *Electrochim. Acta* **2010**, *55*, 8062−8066.
(38) Zheng, W.; Liu, Y.; Hu, X.; Zhang, C. Novel Nanosized Adsorbing Sulfur Composite Cathode Materials for the Advanced Secondary Lithium Batteries. *Electrochim. Acta* **2006**, *51*, 1330−1335.
(39) Hirsch, A. Functionalization of Single-Walled Carbon Nanotubes. *Angew. Chem., Int. Ed.* **2002**, *41*, 1853−1859.
(40) Zhou, G.; Li, L.; Ma, C.; Wang, S.; Shi, Y.; Koratkar, N.; Ren, W.; Li, F.; Cheng, H. A Graphene Foam Electrode with High Sulfur Loading for Flexible and High Energy Li-S Batteries. *Nano Energy* **2015**, *11*, 356−365.

DOI: 10.1021/acsami.7b16174
ACS Appl. Mater. Interfaces 2018, 10, 3938−3947

(41) Wei Seh, Z.; Li, W.; Cha, J.; Zheng, G.; Yang, Y.; McDowell, M.; Hsu, P.; Cui, Y. Sulphur-TiO_2 Yolk-shell Nanoarchitecture with Internal Void Space for Long-cycle Lithium-sulphur Batteries. *Nat. Commun.* **2013**, *4*, 1331−1336.
(42) Xiao, Z.; Yang, Z.; Wang, L.; Nie, H.; Zhong, M.; Lai, Q.; Xu, X.; Zhang, L.; Huang, S. A Lightweight TiO(2)/Graphene Interlayer, Applied as a Highly Effective Polysulfide Absorbent for Fast, Long-Life Lithium-Sulfur Batteries. *Adv. Mater.* **2015**, *27*, 2891−2898.
(43) Yu, M.; Ma, J.; Song, H.; Wang, A.; Tian, F.; Wang, Y.; Qiu, H.; Wang, R. Atomic Layer Deposited TiO_2 on a Nitrogen-doped Graphene/sulfur Electrode for High Performance Lithium−sulfur Batteries. *Energy Environ. Sci.* **2016**, *9*, 1495−1503.
(44) Chen, H.; Dong, W.; Ge, J.; Wang, C.; Wu, X.; Lu, W.; Chen, L. Ultrafine Sulfur Nanoparticles in Conducting Polymer Shell as Cathode Materials for High Performance Lithium/sulfur Batteries. *Sci. Rep.* **2013**, *3*, 1910.
(45) Rehman, S.; Guo, S.; Hou, Y. Rational Design of Si/SiO @ Hierarchical Porous Carbon Spheres as Efficient Polysulfide Reservoirs for High-Performance Li-S Battery. *Adv. Mater.* **2016**, *28*, 3167−3172.
(46) Zhou, W.; Yu, Y.; Chen, H.; DiSalvo, F.; Abruna, H. Yolk-shell Structure of Polyaniline-coated Sulfur for Lithium-sulfur Batteries. *J. Am. Chem. Soc.* **2013**, *135*, 16736−16743.
(47) Li, G.; Sun, J.; Hou, W.; Jiang, S.; Huang, Y.; Geng, J. Three-dimensional Porous Carbon Composites Containing High Sulfur Nanoparticle Content for High-performance Lithium-sulfur Batteries. *Nat. Commun.* **2016**, *7*, 10601−10610.
(48) He, G.; Evers, S.; Liang, X.; Cuisinier, M.; Garsuch, A.; Nazar, L. Tailoring Porosity in Carbon Nanospheres for Lithium Sulfur Battery Cathodes. *ACS Nano* **2013**, *7*, 10920−10930.
(49) Fu, Y.; Su, Y.; Manthiram, A. Highly Reversible Lithium/dissolved Polysulfide Batteries with Carbon Nanotube Electrodes. *Angew. Chem., Int. Ed.* **2013**, *52*, 6930−6935.
(50) Yan, J.; Liu, X.; Qi, H.; Li, W.; Zhou, Y.; Yao, M.; Li, B. High-Performance Lithium−Sulfur Batteries with a Cost-Effective Carbon Paper Electrode and High Sulfur-Loading. *Chem. Mater.* **2015**, *27*, 6394−6401.
(51) Yang, W.; Yang, W.; Song, A.; Gao, L.; Sun, G.; Shao, G. Pyrrole as a Promising Electrolyte Additive to Trap Polysulfides for Lithium-sulfur Batteries. *J. Power Sources* **2017**, *348*, 175−182.
(52) Dorfler, S.; Hagen, M.; Althues, H.; Tubke, J.; Kaskel, S.; Hoffmann, M. High Capacity Vertical Aligned Carbon Nanotube/sulfur Composite Cathodes for Lithium-sulfur Batteries. *Chem. Commun. (Cambridge, U. K.)* **2012**, *48*, 4097−4099.
(53) Su, Y.; Fu, Y.; Manthiram, A. Self-weaving Sulfur-carbon Composite Cathodes for High rate Lithium-sulfur Batteries. *Phys. Chem. Chem. Phys.* **2012**, *14*, 14495−14499.
(54) Guo, J.; Xu, Y.; Wang, C. Sulfur-impregnated Disordered Carbon Nanotubes Cathode for Lithium-sulfur Batteries. *Nano Lett.* **2011**, *11*, 4288−4294.
(55) Zhang, S. Effect of Discharge Cutoff Voltage on Reversibility of Lithium/Sulfur Batteries with LiNO3-Contained Electrolyte. *J. Electrochem. Soc.* **2012**, *159*, A920−A923.
(56) Cao, Z.; Ma, C.; Jia, Y.; Sun, Z.; Yue, H.; Yin, Y.; Yang, S. Activated Clay of Roost Structure Encapsulated Sulfur Cathodes for Lithium−sulfur Batteries. *RSC Adv.* **2015**, *5*, 28349−28353.
(57) Li, W.; Zheng, G.; Yang, Y.; Seh, Z.; Liu, N.; Cui, Y. High-performance Hollow Sulfur Nanostructured Battery Cathode Through a Scalable, Room Temperature, One-step, Bottom-up Approach. *Proc. Natl. Acad. Sci. U. S. A.* **2013**, *110*, 7148−7153.
(58) Deng, Z.; Zhang, Z.; Lai, Y.; Liu, J.; Li, J.; Liu, Y. Electrochemical Impedance Spectroscopy Study of a Lithium/Sulfur Battery: Modeling and Analysis of Capacity Fading. *J. Electrochem. Soc.* **2013**, *160*, A553−A558.
(59) Barchasz, C.; Leprêtre, J.; Alloin, F.; Patoux, S. New Insights Into the Limiting Parameters of the Li/S Rechargeable Cell. *J. Power Sources* **2012**, *199*, 322−330.
(60) Yuan, L.; Qiu, X.; Chen, L.; Zhu, W. New Insight Into the Discharge Process of Sulfur Cathode by Electrochemical Impedance Spectroscopy. *J. Power Sources* **2009**, *189*, 127−132.
(61) Hua, W.; Yang, Z.; Nie, H.; Li, Z.; Yang, J.; Guo, Z.; Ruan, C.; Chen, X.; Huang, S. Polysulfide-Scission Reagents for the Suppression of the Shuttle Effect in Lithium-Sulfur Batteries. *ACS Nano* **2017**, *11*, 2209−2218.
(62) Lv, D.; Zheng, J.; Li, Q.; Xie, X.; Ferrara, S.; Nie, Z.; Mehdi, L.; Browning, N.; Zhang, J.; Graff, G.; Liu, J.; Xiao, J. High Energy Density Lithium-Sulfur Batteries: Challenges of Thick Sulfur Cathodes. *Adv. Energy Mater.* **2015**, *5*, 1402290.
(63) Zhou, G.; Pei, S.; Li, L.; Wang, D.; Wang, S.; Huang, K.; Yin, L.; Li, F.; Cheng, H. A Graphene-Pure-Sulfur Sandwich Structure for Ultrafast, Long-Life Lithium-Sulfur batteries. *Adv. Mater.* **2014**, *26*, 625−631.
(64) Hu, C.; Kirk, C.; Cai, Q.; Cuadrado-Collados, C.; Silvestre-Albero, J.; Rodriguez-Reinoso, F.; Biggs, M. A High-Volumetric-Capacity Cathode Based on Interconnected Close-Packed N-Doped Porous Carbon Nanospheres for Long-Life Lithium-Sulfur Batteries. *Adv. Energy Mater.* **2017**, *7*, 1701082−1701091.

DOI: 10.1021/acsami.7b16174
ACS Appl. Mater. Interfaces 2018, 10, 3938−3947